RSC Sustainability

ROYAL SOCIETY OF CHEMISTRY

COMMUNICATION

View Article Online
View Journal | View Issue

Check for updates

Cite this: *RSC Sustainability*, 2026, **4**, 221

Received 28th October 2025
Accepted 31st October 2025

DOI: 10.1039/d5su00828j

rsc.li/rscsus

Open Access Article. Published on 31 10 2025. Downloaded on 2026/05/27 7:47:24.
This article is licensed under a Creative Commons Attribution 3.0 Unported Licence.

Vitrimers from non-functionalized lignin oil and epoxidized soybean oil

Ella F. Clark, †[a] Tripti Chhabra, †[a] Qianxiang Zhou,[a] Niklas Lorenz,[b] Jonathan Woods,[a] Peter Van Puyvelde,[c] Baris Kumru[b] and Bert F. Sels *[a]

This study reports the development of fully bio-based epoxy resins containing dynamic ester bonds capable of transesterification at 100 °C. The inherent functionality of lignin oil, derived from the reductive catalytic fractionation (RCF) biorefinery process, enables effective curing with epoxidized soybean oil, eliminating the need for additional treatments. The resulting epoxy resins show similar thermochemical behavior for both pristine and reprocessed epoxy resins. This work highlights a sustainable and efficient route for producing reprocessable vitrimers using non-functionalized lignin oil.

Sustainability spotlight

This work presents a simple and detailed study on epoxy resins prepared entirely from bio-based lignin oil and epoxidized soybean oil. These materials replace the toxic, non-recyclable bisphenol A and epichlorohydrin traditionally derived from petrochemical sources. Our vitrimer system utilizes lignin oil with inherently sufficient phenolic and aliphatic hydroxyl groups, eliminating additional functionalization steps. This simplifies the overall process, reducing both cost and time requirements. Our future research will focus on exploring variations in lignin oil composition and their reactivity toward epoxy resins, with particular emphasis on enhancing sustainability and minimizing waste generation during epoxy resin preparation.

Introduction

Epoxy resins are a class of thermoset materials with a wide application scope, such as in household items, aerospace, transportation, infrastructure and electrical equipment.[1,2] This is due to their excellent properties, namely high chemical resistance, thermal stability and mechanical strength and suitability for electrical insulation. Often derived from petroleum sources, their inert cross-linked structure does not allow for reprocessing, recycling or degradation.[3] To move towards a more sustainable material whilst maintaining the desirable properties, bioderived monomers with low toxicity must be used to create a material capable of being reprocessed. Covalent adaptable networks (CANs) possess dynamic covalent bonds, which can be broken and reformed, resulting in a material with macroscopic flow capable of being reprocessed.[4–6] Dynamic bonding, such as transesterification, can be introduced into epoxy resins through the choice of hardener to form a vitrimer.[7–13] For example, Ju and co-workers reacted tannic acid with epoxidized vegetable oils to produce epoxy resins with good reprocessability and robust mechanical properties.[14]

Biomass is currently the most abundant renewable and biodegradable resource on our planet and a good alternative to petroleum-based products.[15] Lignin is the second most abundant polymer present in biomass. It is naturally rich in aromatic units, which are present in plant structures.[16–18] Numerous chemical processes have been extensively studied for the isolation of lignin from the lignocellulosic biomass. Kraft, sulfite, alkaline and klason lignin are typically obtained from the pulping methods. While these processes yield high quality cellulose, the lignin produced is highly modified from its native structure due to harsh chemical treatment. Milled wood lignin, obtained by intensive grinding followed by solvent treatment, also results in structurally altered lignin. The organosolv process and ionic liquid method are also used to obtain lignin. In the organosolv process, structurally modified lignin is obtained if treated at high temperature, and the ionic liquid method is not cost effective.[19] Therefore, valorization of lignocellulosic biomass to obtain structurally unmodified lignin in an economically viable manner remains a significant challenge.[20] Reductive catalytic fractionation (RCF) is a promising one pot technique and is often referred to as a "lignin first-biorefinery" approach. The RCF process enables the efficient separation of carbohydrate pulp and lignin oil through

[a]*Center For Sustainable Catalysis and Engineering, Department of Microbial and Molecular Systems, KU Leuven, Leuven, Belgium. E-mail: bert.sels@kuleuven.be*

[b]*Faculty of Aerospace Engineering, Aerospace Structures & Materials Department, Delft University of Technology, 2629 HS Delft, Netherlands*

[c]*Department of Chemical Engineering, Soft Matter, Rheology and Technology (SMaRT), KU Leuven, Celestijnenlaan 200F, 3001 Leuven, Belgium*

† These authors contributed equally to this work.

© 2026 The Author(s). Published by the Royal Society of Chemistry

Open Access Article. Published on 31 10 2025. Downloaded on 2026/05/27 7:47:24.
This article is licensed under a Creative Commons Attribution 3.0 Unported Licence.

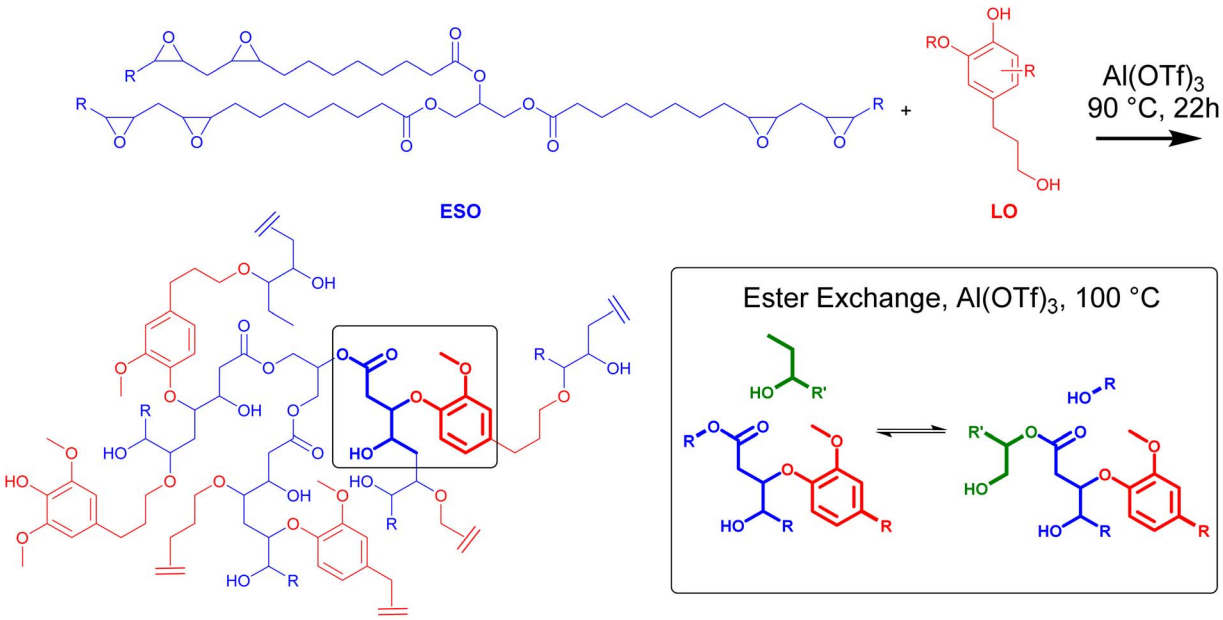

Scheme 1 Illustration of the reaction of LO and ESO with $Al(OTf)_3$ at 90 °C, resulting in an epoxy resin. Dynamic bonding occurs between ester and alcohol groups (transesterification), catalyzed by $Al(OTf)_3$ at 100 °C.

a straightforward chemical process. Lignin oil obtained *via* RCF comprises a mixture of phenolic monomers, dimers and oligomers, preserving lignin in its native and unaltered form.[19,21]

The dynamic structure of lignin consists of different active functional groups such as hydroxyl, methoxy, aldehyde and carboxylic. This allows lignin to undergo a range of chemical modifications such as alcoholysis, oxidation, reduction, epoxidation and demethoxylation.[22] This modified structure of lignin can be used to develop new materials with improved reprocessability, improved mechanical properties, and environmental sustainability.[23]

Zhang and coworkers used the commercially available kraft lignin which was further subjected to ozone oxidation for cleavage of the lignin structure and also to increase the carboxylic groups in the lignin. The modified lignin was used to prepare the vitrimers with sebacic acid for reprocessable adhesives.[24] Recently, Duval *et al.* used the commercial kraft lignin and treated it with ethylene carbonate to increase the aliphatic hydroxyl groups present in the lignin. The modified kraft lignin was further crosslinked with poly(ethylene glycol) bis(carboxymethyl) ether to form lignin based polyester networks.[25] Wang *et al.*[26] reported the development of epoxy resins from kraft lignin and epoxidized soybean oil (ESO). However, the inherent polarity and hydrophilicity of lignin oppose the hydrophobic nature of ESO, which leads to a compatibility issue. To enhance the compatibility between lignin and ESO, lignin underwent esterification with tung oil anhydride to enhance its compatibility with ESO prior to epoxy resin synthesis. There is a need to prepare the structurally unmodified lignin with high phenolic and aliphatic hydroxyl content for the synthesis of vitrimer materials.

This work explores the potential of unmodified lignin oil obtained from RCF,[21,27] an emerging lignocellulose biorefinery that focusses on extraction of high quality lignin oil, to develop sustainable and bio-based epoxy vitrimers (Scheme 1). The aliphatic and phenolic OH groups present in the lignin oil are reacted with ESO to form an epoxy resin. Once cured, these resins resulted in bio-based thermosets which are studied for their dynamic bonding and reprocessibility.

Results and discussion

Lignin oil, rich in both aliphatic and phenolic hydroxyl groups, was obtained *via* the RCF process and used directly without further chemical modification (see the SI for details). The weight-average molar mass (M_w) of LO was found to be 2159 g mol^{-1} as determined from GPC, which is shown in Fig. S1. The quantitative analysis of aliphatic and phenolic hydroxyl groups present in LO was determined by $^{31}P\{^1H\}$ NMR analysis. The G unit (guaiacyl), S unit (syringyl) along with condensed structures and H unit (hydroxyphenyl) were calculated to be 0.82 mmol g^{-1}, 1.94 mmol g^{-1} and 0.13 mmol g^{-1}, respectively. The total amount of aliphatic and phenolic hydroxylic groups was found to be 1.94 mmol g^{-1} and 2.89 mmol g^{-1}, respectively. The 2D ^1H–^{13}C HSQC NMR spectra were further used to elucidate the fragments and their relative percentage present in the LO, as presented in Fig. 1(a, b and e), which were measured in DMSO-d_6. The main structural units found in LO were Me, E, and P with relative amounts of 0.6%, 13.4%, and 12.7%, respectively. The P γ-OH structural unit was found to be 29.8%, which confirms the high aliphatic hydroxyl group content in the LO. The other structures present in LO were P γ-OMe (8.8%) and α,β β-1E (3.6%) along with $-OCH_3$ and $ROOCH_3$ functional groups.[28]

The optimization of curing ESO with LO was next carried out. Catalyst screening was performed *via* DSC analysis, identifying

© 2026 The Author(s). Published by the Royal Society of Chemistry

Open Access Article. Published on 31 10 2025. Downloaded on 2026/05/27 7:47:24.
This article is licensed under a Creative Commons Attribution 3.0 Unported Licence.

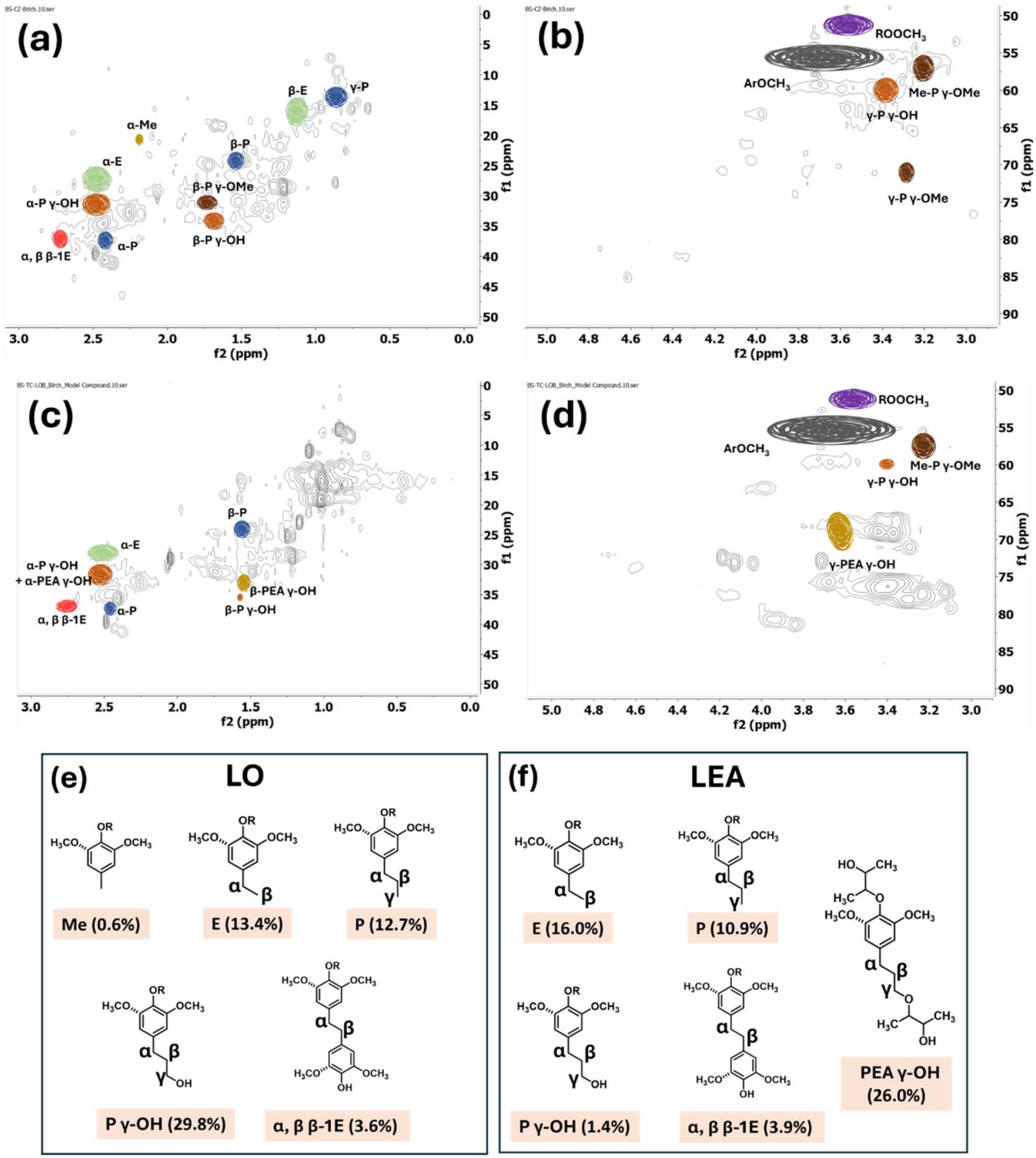

Fig. 1 2D (^{1}H–^{13}C) HSQC NMR spectra of (a and b) LO and (c and d) LEA. Relative quantification of structures in (e) LO and (f) LEA.

curing by measuring exothermic events caused by the ring-opening of the epoxide. Analysis was done at a weight/weight% ratio (w/w%) with LO/ESO w/w% of 24% and catalyst/ESO w/w% of 1% to ensure the epoxide was in excess. Three catalysts, zinc acetate ($ZnAc_2$), aluminium trifluoromethanesulfonate $Al(OTf)_3$ and histidine, were all chosen, having all been reported to catalyse epoxy curing and dynamic ester exchange.[8,29–31] Although $ZnAc_2$ produced a minor exothermic event, the largest exotherm was produced by $Al(OTf)_3$ with a peak exothermic temperature at 109 °C (Fig. S4). Film formulation was next optimized in a PTFE mold. Initial upscaling was done with 2.00 g of ESO with LO/ESO w/w% of 24% and $Al(OTf)_3$/ESO w/w% of 1% at 90 °C in an oven. The temperature was varied across the exothermic range from

Open Access Article. Published on 31 10 2025. Downloaded on 2026/05/27 7:47:24.
This article is licensed under a Creative Commons Attribution 3.0 Unported Licence.

Table 1 Film optimization

Entry[a]	LO/ESO w/w%	Curing time (h)	Curing temp (°C)	cat/ESO w/w%	T_g[b]	$T_{d,5\%}$[c]
1	24	22	120	1.00	−39	239
2	24	22	105	1.00	−38	241
3	24	22	90	1.00	−35	228
4	24	5	90	1.00	−36	219
5	24	3	90	1.00	−40	195
6	24	1	90	1.00	−43	206
7	24	22	90	0.50	−36	243
8	24	22	90	0.25	−34	266
9	18	4	90	0.50	−37	222
10	28	4	90	0.50	−35	224
11	24	22	90	0	—	—
12	24	28	180	0	—	—

[a] Reactions carried out with $Al(OTf)_3$. [b] Values taken from the second heating cycle. [c] Value taken at 5% mass loss.

120 to 90 °C (Table 1, entries 1–3). Curing at 90 °C produced a homogeneous film unlike higher temperatures in which bubbling occurred, likely due to rapid curing. After 22 h, the film had solidified and was removed from the mold. The disappearance of the epoxy ν_{C-O} vibration between 800 and 850 cm^{-1} in the Fourier-transform infrared spectrscopy (FT-IR) spectrum suggested high consumption of epoxy groups (Fig. S7). No residual curing exotherm was observed by DSC analysis for any of the films after curing, confirming all films were fully cured. Solidification occurred after only 1 h, and FT-IR analysis confirmed the film was fully cured. The catalyst loading for $Al(OTf)_3$/ESO (w/w%) was further decreased to 0.5% and 0.25% (Table 1, entries 7–9). Curing occurred at all loadings, as evidenced by solidification and disappearance of the ν_{C-O} vibration in the FT-IR spectrum. A significant increase in $T_{d,5\%}$ with decreased catalyst loading was observed, suggesting that $Al(OTf)_3$ catalyzes the degradation of the epoxy resin. Finally, the w/w% of LO/ESO was varied (Table 1, entries 9 and 10). The $T_{d,5\%}$ decreased with increasing lignin content (Fig. S5) with the T_g remaining between −36 and −32 °C. The DSC trace of all films also exhibited an endotherm between −20 and 0 °C, which was attributed to the melting of ESO (Fig. S6).

To gain further insights into the resin formulation, *trans*-2,3-epoxybutane was chosen as a model epoxide compound for better understanding the reactivity of LO and epoxide. Studying the reaction of LO with *trans*-2,3-epoxybutane helps in identifying which functional groups present in LO participate in the curing reaction. The chemical reaction between LO and *trans*-2,3-epoxybutane resulted in the lignin–epoxy adduct (LEA). The formation of LEA resulted in an increase in M_w from 2159 g mol^{-1} to 3385 g mol^{-1}, as shown in Fig. S1, indicating that the epoxide has successfully reacted with the lignin oil. The $^{31}P\{^1H\}$ NMR analysis confirmed an increase in aliphatic hydroxyl content from 1.94 mmol g^{-1} in LO to 2.61 mmol g^{-1} in LEA, as shown in Fig. S2 and Table S1. A corresponding decrease from 2.89 mmol g^{-1} to 1.02 mmol g^{-1} in phenolic hydroxyl groups was also observed, signifying that the addition of *trans*-2,3-epoxybutane at the phenolic position resulting in the formation of aliphatic hydroxyl groups. These observations suggest that the epoxide reacts with both aliphatic and phenolic hydroxyl functional groups, which are present among the various structural motifs present in lignin oil.

Furthermore, propanol guaiacol (PG) was chosen as a model compound for lignin to understand the reactivity of epoxide with aliphatic hydroxyl and phenolic groups present in LO. PG was next reacted with *trans*-2,3-epoxybutane to form the PG–epoxy adduct (PGEA) as a model product. The $^1H-^{13}C$ HSQC spectrum and relative quantification of PGEA are provided in Fig. S3 and Table S2. The $^1H-^{13}C$ HSQC spectrum of PGEA shows that the signal for the α-position of both PG and PGEA remained at 2.5 ppm, whereas a shift in the signals corresponding to the β- and γ-positions was observed for PG and PGEA, which confirm the addition of *trans*-2,3-epoxybutane and also provide the relative quantification of epoxidation. $PGEA_1$ and $PGEA_2$ were attributed to the addition of *trans*-2,3-epoxybutane at the phenolic hydroxyl position, and $PGEA_3$ and $PGEA_4$ were attributed to the addition of *trans*-2,3-epoxybutane at the aliphatic hydroxyl position. The higher relative percentages of $PGEA_3$ and $PGEA_4$ compared to $PGEA_1$ and $PGEA_2$ (Table S2) suggest that addition of *trans*-2,3-epoxybutane is more favorable at aliphatic hydroxyl sites than at phenolic positions.

The $^1H-^{13}C$ HSQC spectra and relative quantification of LEA are shown in Fig. 1(c, d and f). Signals for the α-position in both P γ-OH and PEA γ-OH appear at the same location, while the β- and γ-positions for P γ-OH and PEA γ-OH differ, enabling the calculation of the extent of *trans*-2,3-epoxybutane addition. The relative amount of P γ-OH decreases from 29.8% to 1.4%, while PEA γ-OH accounts for 26.0%, which confirm the successful addition to lignin oil. However, due to signal clustering in the PEA γ-OH region, specific assignments are uncertain. Unlike the clear preference for addition of *trans*-2,3-epoxybutane at aliphatic hydroxyl groups observed in the PG–epoxy adduct, the data for the lignin–epoxy adduct do not allow for a definitive conclusion regarding the reactivity of aliphatic *versus* phenolic hydroxyl groups. The chemical reactivity of *trans*-2,3-epoxybutane with PG and LO indicates that addition of epoxy functional groups takes place at both aliphatic and phenolic positions in various structures present in lignin oil, with higher

© 2026 The Author(s). Published by the Royal Society of Chemistry

Open Access Article. Published on 31 10 2025. Downloaded on 2026/05/27 7:47:24.
This article is licensed under a Creative Commons Attribution 3.0 Unported Licence.

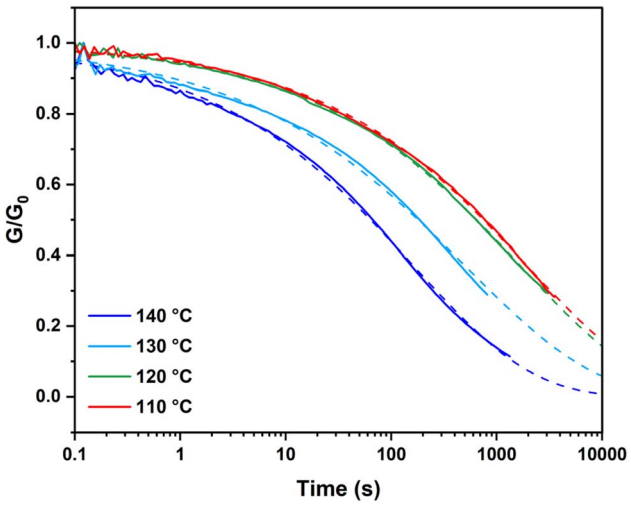

Fig. 2 Normalized relaxation modulus (solid line) and approximation using the Kohlrausch–Williams–Watts function (dotted line) at different temperatures.

reactivity observed at the aliphatic position compared to the phenolic position.

Dynamic bond exchange

Vitrimers show that the stress caused by deformation can be released at high temperatures through dynamic cross-linking exchange. To establish whether the network behaves as a vitrimer, shear stress-relaxation experiments were performed between 110 and 140 °C on an epoxy resin (LO/ESO w/w% of 24% and $Al(OTf)_3$/ESO w/w% of 1%, cured at 90 °C). The shear relaxation modulus $G(t)$ was measured as a function of time at each temperature. A decrease in relaxation time was observed as the temperature was increased from 110 to 140 °C (Fig. 2). Normalized shear modulus data were approximated using Kohlrausch–Williams–Watts stretched exponential decay to obtain the average relaxation time $\langle\tau\rangle$ (refer to the SI).[32,33] Low values of $\langle\tau\rangle$ (Fig. S12) indicate rapid stress relaxation behaviour and excellent dynamic properties, while stretching coefficient β values ranging from 0.35 to 0.38 suggest an inhomogeneous relaxation process, which may be attributed to the inhomogeneous structure of LO. For the LO-derived epoxy resins, $\langle\tau\rangle$ was shown to be less than 600 seconds at 140 °C, with an activation energy of 112 kJ mol^{-1}, which falls within the range of transesterification vitrimers[34,35] between 85 and 129 kJ mol^{-1}.

The reprocessing capability was next explored. An epoxy resin was formulated at a LO/ESO w/w% of 24% and $Al(OTf)_3$/ESO w/w% of 1% at 90 °C. A fracture was introduced into the epoxy resin using a knife and subsequently characterized using Scanning Electron Microscopy (SEM) (Fig. 3(a, b)). Following compression molding at 100 °C for 3 h at 50 bar pressure, no fracture was observed *via* SEM, demonstrating the film's ability to be reprocessed (Fig. 3(c and d) and S13).

Samples for Dynamic Mechanical Analysis (DMA) were prepared by cleaving a 62.5 × 12.5 mm bar into two followed by compression molding at 100 °C for 3 h. These were compared to pristine samples (uncut, cured epoxy resins) of the same dimension. Fig. 3(e) shows the temperature-dependent modulus of the pristine and reprocessed samples, confirming similar thermomechanical behavior of both samples. A broad glass transition temperature, T_g, of −7.5 °C (tan(δ) peak value) remains constant before and after the thermal reprocessing, indicating no undesired degradation by bond breakage during reprocessing, which would manifest in decreasing T_g values.[36,37] The master curves of the pristine and reprocessed materials at a reference temperature of 20 °C (Fig. S14) show similar behavior over a wide frequency range, indicating preservation of thermomechanical properties during the reprocessing. Furthermore, the shift factors a_T derived from the loss factor tan δ (Fig. S15) confirm similar behavior of pristine and

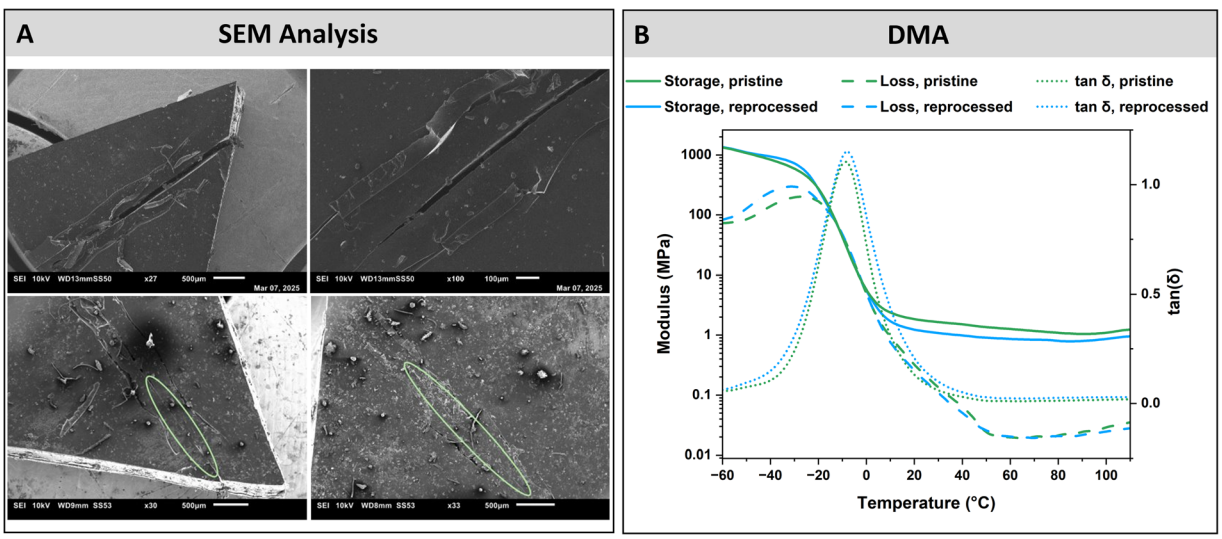

Fig. 3 SEM images of the (a and b) freshly cut polymeric film and (c and d) compression molded polymeric film. The scale bars for the SEM images are 500 μm for (a and c) and 100 μm for (b and d). (e) DMA temperature ramp profiles of pristine and reprocessed samples.

Open Access Article. Published on 31 10 2025. Downloaded on 2026/05/27 7:47:24.
This article is licensed under a Creative Commons Attribution 3.0 Unported Licence.

reprocessed samples. This shows the overall viscoelastic response of the reprocessed specimen does not significantly differ between the pristine and reprocessed samples. Moreover, the glassy regime falls within the range of similar epoxy vitrimers derived from functionalized lignin[25,38–40] as well as existing commercial epoxy resins.

Conclusions

The formulation of fully biobased epoxy resins from unfunctionalized LO and ESO has been reported. DSC curing analysis found $Al(OTf)_3$ to be an effective catalyst, which was further corroborated by $^{31}P\{^1H\}$ and ^1H–^{13}C HSQC NMR analysis which showed that $Al(OTf)_3$ catalyzed the ring-opening attack of epoxides by LO, with preference to aliphatic hydroxyl groups. Having optimized film formulation, rheology, SEM and DMA experiments were then performed to show that these epoxy resins undergo dynamic bond exchange and are capable of being reprocessed with pristine and reprocessed films exhibiting the same viscoelastic properties.

Conflicts of interest

There are no conflicts to declare.

Data availability

All data supporting the findings of this study are available. All the findings are included in the article and its supporting information (SI). Full experimental procedures are provided in the SI. Supplementary information is available. See DOI: **https://doi.org/10.1039/d5su00828j**.

Acknowledgements

This project received financial support from the Internal KU Leuven research fund for the GORILLA project (C2M/23/025), FWO Strategic research project LigDYN (S000724N) and Next-BIOREF (IBOF/21/105).

References

1 Y. Jiang, J. Li, D. Li, Y. Ma, S. Zhou, Y. Wang and D. Zhang, *Chem. Soc. Rev.*, 2024, **53**, 624–655.
2 A. Shundo, S. Yamamoto and K. Tanaka, *JACS Au*, 2022, **2**, 1522–1542.
3 M. Peerzada, S. Abbasi, K. T. Lau and N. Hameed, *Ind. Eng. Chem. Res.*, 2020, **59**, 6375–6390.
4 C. J. Kloxin and C. N. Bowman, *Chem. Soc. Rev.*, 2013, **42**, 7161–7173.
5 X.-L. Zhao, P.-X. Tian, Y.-D. Li and J.-B. Zeng, *Green Chem.*, 2022, **24**, 4363–4387.
6 F. Zhang, L. Zhang, M. Yaseen and K. Huang, *J. Appl. Polym. Sci.*, 2021, **138**, 50260.
7 P. Verdugo, D. Santiago, S. De la Flor and À. Serra, *ACS Sustain. Chem. Eng.*, 2024, **12**, 5965–5978.
8 Y. Tao, L. Fang, M. Dai, C. Wang, J. Sun and Q. Fang, *Polym. Chem.*, 2020, **11**, 4500–4506.
9 E. Albertini, S. Dalle Vacche, R. Bongiovanni, I. Bianco, G. A. Blengini and A. Vitale, *ACS Sustain. Chem. Eng.*, 2025, **13**, 2120–2131.
10 M. Comí, B. Van Ballaer, J. Gracia-Vitoria, D. Parida, A. Aerts, K. Vanbroekhoven and R. Vendamme, *ACS Sustain. Chem. Eng.*, 2024, **12**, 9279–9289.
11 H. Yao, H. Yang, L. Jiang, W. Huang, Q. Jiang, B. Jiang and G. Zhang, *RSC Appl. Polym.*, 2025, **3**, 163–172.
12 J. Zhang, Z. Gong, C. Wu, T. Li, Y. Tang, J. Wu, C. Jiang, M. Miao and D. Zhang, *Green Chem.*, 2022, **24**, 6900–6911.
13 D. Montarnal, M. Capelot, F. Tournilhac and L. Leibler, *Science*, 2011, **334**, 965–968.
14 J. Li, B. Ju and S. Zhang, *Green Chem.*, 2024, **26**, 7113–7122.
15 B. H. H. Goh, H. C. Ong, M. Y. Cheah, W.-H. Chen, K. L. Yu and T. M. I. Mahlia, *Renewable Sustainable Energy Rev.*, 2019, **107**, 59–74.
16 A. J. Ragauskas, G. T. Beckham, M. J. Biddy, R. Chandra, F. Chen, M. F. Davis, B. H. Davison, R. A. Dixon, P. Gilna, M. Keller, P. Langan, A. K. Naskar, J. N. Saddler, T. J. Tschaplinski, G. A. Tuskan and C. E. Wyman, *Science*, 2014, **344**, 1246843.
17 E. Sheridan, S. Filonenko, A. Volikov, J. Antti Sirviö and M. Antonietti, *Green Chem.*, 2024, **26**, 2967–2984.
18 Y. Liao and B. F. Sels, *Lignin Chemistry: Characterization, Isolation, and Valorization*, John Wiley & Sons, 2024.
19 Z. Sun, B. Fridrich, A. de Santi, S. Elangovan and K. Barta, *Chem. Rev.*, 2018, **118**, 614–678.
20 Y. Huang, Y. Duan, S. Qiu, M. Wang, C. Ju, H. Cao, Y. Fang and T. Tan, *Sustain. Energy Fuels*, 2018, **2**, 637–647.
21 S. Van Den Bosch, W. Schutyser, R. Vanholme, T. Driessen, S.-F. Koelewijn, T. Renders, B. De Meester, W. J. J. Huijgen, W. Dehaen, C. M. Courtin, B. Lagrain, W. Boerjan and B. F. Sels, *Energy Environ. Sci.*, 2015, **8**, 1748–1763.
22 N. Sun, Z. Wang, X. Ma, K. Zhang, Z. Wang, Z. Guo, Y. Chen, L. Sun, W. Lu and Y. Liu, *Ind. Crops Prod.*, 2021, **174**, 114178.
23 R. Tang, B. Xue, J. Tan, Y. Guan, J. Wen, X. Li and W. Zhao, *ACS Appl. Polym. Mater.*, 2022, **4**, 1117–1125.
24 S. Zhang, T. Liu, C. Hao, L. Wang, J. Han, H. Liu and J. Zhang, *Green Chem.*, 2018, **20**, 2995–3000.
25 A. Duval, W. Benali and L. Avérous, *Green Chem.*, 2024, **26**, 8414–8427.
26 X. Zhen, X. Cui, A. A. N. M. Al-Haimi, X. Wang, H. Liang, Z. Xu and Z. Wang, *Int. J. Biol. Macromol.*, 2024, **254**, 127760.
27 M. Chen, Y. Li, F. Lu, J. S. Luterbacher and J. Ralph, *ACS Sustain. Chem. Eng.*, 2023, **11**, 10001–10017.
28 K. V. Aelst, E. V. Sinay, T. Vangeel, E. Cooreman, G. V. den Bossche, T. Renders, J. V. Aelst, S. V. den Bosch and B. F. Sels, *Chem. Sci.*, 2020, **11**, 11498–11508.
29 D. B. G. Williams and M. Lawton, *Org. Biomol. Chem.*, 2005, **3**, 3269–3272.
30 I. D. S. Silva, P. Moerbitz, I. Bretz, J. V. Barreto, A. Ries, C. B. B. Luna, E. M. Araújo and R. M. R. Wellen, *J. Appl. Polym. Sci.*, 2025, **142**, e56908.
31 M. Shibata, J. Fujigasaki, M. Enjoji, A. Shibita, N. Teramoto and S. Ifuku, *Eur. Polym. J.*, 2018, **98**, 216–225.

© 2026 The Author(s). Published by the Royal Society of Chemistry

32 G. Williams and D. C. Watts, *Trans. Faraday Soc.*, 1970, **66**, 80–85.
33 N. Lorenz, W. E. Dyer and B. Kumru, *J. Polym. Sci.*, 2025, **63**, 3739–3751.
34 M. Chen, H. Si, H. Zhang, L. Zhou, Y. Wu, L. Song, M. Kang and X.-L. Zhao, *Macromolecules*, 2021, **54**, 10110–10117.
35 M. Capelot, M. M. Unterlass, F. Tournilhac and L. Leibler, *ACS Macro Lett.*, 2012, **1**, 789–792.
36 N. Lorenz, W. E. Dyer and B. Kumru, *ACS Appl. Polym. Mater.*, 2025, **7**, 1934–1946.
37 A. Ruiz de Luzuriaga, N. Markaide, A. M. Salaberria, I. Azcune, A. Rekondo and H. J. Grande, *Polymers*, 2022, **14**, 3180.
38 F. Meng, M. O. Saed and E. M. Terentjev, *Nat. Commun.*, 2022, **13**, 5753.
39 A. Duval, W. Benali and L. Avérous, *ChemSusChem*, 2025, **18**, e202401480.
40 R. Chen, L. Zhou, K. Zhang and M. Chen, *J. Appl. Polym. Sci.*, 2024, **141**, e55655.

Open Access Article. Published on 31 10 2025. Downloaded on 2026/05/27 7:47:24.
This article is licensed under a Creative Commons Attribution 3.0 Unported Licence.